MOLECULAR AND CELLULAR BIOLOGY, Feb. 2005, p. 1339–1346 Vol. 25, No. 4
0270-7306/05/$08.00+0 doi:10.1128/MCB.25.4.1339–1346.2005

Unchanged Survival Rates of 14-3-3γ Knockout Mice after Inoculation with Pathological Prion Protein

Petra Steinacker,[1]* Petra Schwarz,[2] Kerstin Reim,[3] Peter Brechlin,[1] Olaf Jahn,[3] Hartmut Kratzin,[4] Alastair Aitken,[5] Jens Wiltfang,[6] Adriano Aguzzi,[2] Erik Bahn,[7] Helen C. Baxter,[5] Nils Brose,[3] and Markus Otto[1,8]*

Departments of Neurology,[1] Neuropathology,[7] and Psychiatry,[8] Georg-August University Goettingen, and Departments of Molecular Neurobiology[3] and Neurogenetics,[4] Max Planck Institute for Experimental Medicine, Goettingen, and Department of Psychiatry, Friedrich-Alexander University Erlangen-Nürnberg, Erlangen,[6] Germany; Institute of Neuropathology, University Hospital of Zurich, Zurich, Switzerland[2]; and School of Biomedical and Clinical Laboratory Sciences, University of Edinburgh, Edinburgh, United Kingdom[5]

Received 5 April 2004/Returned for modification 28 May 2004/Accepted 4 October 2004

The diagnosis of sporadic Creutzfeldt-Jakob disease (CJD) is based on typical clinical findings and is supported by a positive 14-3-3 Western blot of cerebrospinal fluid. However, it is not clear whether 14-3-3 indicates general neuronal damage or is of pathophysiological relevance in CJD. The fact that the 14-3-3 isoform spectrum in cerebrospinal fluid does not correspond to that found in the brain points to a regulated process. To investigate a possible role of 14-3-3 proteins in transmissible spongiform diseases, we generated a 14-3-3γ-deficient mutant mouse line by using a classical knockout strategy. The anatomy and cage behavior of the mutant mice were normal. Western blot analyses of brain homogenates revealed no changes in the protein expression of other 14-3-3 isoforms (ε, β, ζ, and η). Proteomic analyses of mouse brains by two-dimensional differential gel electrophoresis showed that several proteins, including growth hormone, 1-Cys peroxiredoxin, CCT-zeta, glucose-6-phosphate isomerase, GRP170 precursor, and α-SNAP, were differentially expressed. Mutant and wild-type mice were inoculated either intracerebrally or intraperitoneally with the Rocky Mountain Laboratory strain of scrapie, but no differences were detected in the postinoculation survival rates. These results indicate that 14-3-3γ is unlikely to play a causal role in CJD and related diseases.

14-3-3 proteins are a family of highly homologous, ubiquitously expressed isoforms that are involved in a wide variety of physiological processes, including neuronal development, apoptosis, cell cycle control, and signal transduction. The extraordinary large number of 14-3-3 binding partners—more than 100 have been reported—suggests a role of 14-3-3 isoforms as general regulatory proteins (reviewed in references 1, 4, 14, and 41). Mammals express seven distinct 14-3-3 isoforms (γ, ε, β, ζ, η, σ, and τ) which comprise 1% of the total amount of soluble brain protein (6). Proteins of the 14-3-3 family have been suggested to play a role in several neurological disorders as a degeneration marker as well as in the actual disease process (13, 20, 25, 31, 46). In particular, in spinocerebellar ataxia, which is a "protein-folding disease," a pivotal role for 14-3-3 proteins has been discovered (10). In sporadic Creutzfeldt-Jakob disease (CJD), another protein-folding disease, the diagnosis is based on clinical findings and can be supported by a positive 14-3-3 Western blot of cerebrospinal fluid (22). However, it is not clear whether there is a functional relationship between 14-3-3 proteins and the pathogenesis of spongiform encephalopathies.

To investigate a possible relationship, we generated a 14-3-3γ-deficient mutant mouse line. We chose 14-3-3γ because this isoform is one of the most abundant isoforms in the brain (29) and the most abundant isoform in the cerebrospinal fluid of CJD patients (45). Knockout and control mice were inoculated intraperitoneally and intracerebrally with the Rocky Mountain Laboratory (RML) strain of scrapie to study a potential role of 14-3-3γ in the pathogenesis of prion disease.

Since 14-3-3γ knockout mice display no obvious alterations in their phenotype, we characterized these mice in more detail. We used Western blot analysis to search for differences in the expression patterns of specific proteins that are involved in vesicle trafficking, neuronal migration, and apoptosis and applied a proteomic approach to identify novel differentially expressed proteins.

MATERIALS AND METHODS

Generation of 14-3-3γ-deficient mice. The 14-3-3γ cDNA was used to screen a 129SV mouse genomic lambda FIXII library (Stratagene) at high stringency. DNA of positive clones was isolated, subcloned into pBluescript (Stratagene), and analyzed by sequencing. A 17.5-kb genomic clone was used to construct the 14-3-3γ targeting vector (see Fig. 1).

The linearized DNA of the 14-3-3γ targeting vector was electroporated into embryonic stem cells (E14), colonies were selected with G418 and 1-2′-deoxy-2′-fluoro-β-D-arabinofuranosyl-5-iodouracil (FIAU), and doubly resistant clones were analyzed by Southern blotting (see Fig. 1). Clones containing a homologously recombined gene were expanded and injected into mouse blastocysts to obtain highly chimeric mice that transmitted the mutation through the germ line. This was confirmed by Southern blotting (genomic DNA) and immunoblotting (brain extracts). Subsequently, genotyping was performed by PCR (see Fig. 2).

Western blot analysis. For Western blot analysis, whole mouse brain was prepared, homogenized in phosphate-buffered saline (1 ml/0.1 g of tissue) containing aprotinin (1 μg/ml), phenylmethylsulfonyl fluoride (0.2 mM) and leupep-

* Corresponding author. Mailing address: Neurologische Klinik und Poliklinik, Georg-August-Universität Göttingen, Robert-Koch-Straße 40, 37075 Göttingen, Germany. Phone: 49-551-39-12905. Fax: 49-551-39-14449. E-mail for Markus Otto: motto@gwdg.de. E-mail for Petra Steinacker: psteina@gwdg.de.

tin (0.5 μg/ml), and sonicated for 30 s. After centrifugation at 20,000 × *g* for 10 min at 4°C, the supernatant was retained and the protein concentration was determined by the bicinchoninic acid assay (Pierce). Brain preparations (10 to 20 μg of total protein) were separated by sodium dodecyl sulfate-polyacrylamide gel electrophoresis (SDS-PAGE) (23) and blotted to polyvinylidene difluoride membranes (semidry) for 30 min at 48 mA. For Western blot detection, the membranes were blocked for 30 min in Tris-buffered saline (TBS)–0.075% Tween 20 containing 5% dry milk and 5% goat serum and incubated with specific primary antibodies (14-3-3-γ1005, 14-3-3-ε_{ct}, 14-3-3-β199, 14-3-3-ζ1002, and 14-3-3-η2 [45]; CDK5 [C-8], and p35 [C-19] from Santa Cruz; BAD and Bcl2 from R&D Systems; Akt and pAkt from Cell Signaling; all others from Synaptic Systems) diluted in blocking buffer, followed by the respective horseradish peroxidase-conjugated secondary antibody. Immunoreactive proteins were visualized by enhanced chemiluminescence (ECL Plus system; Amersham Biosciences); and bands were quantified using Quantity One software (Bio-Rad).

Histological methods. Formalin-fixed brain tissue of 14-3-3γ-deficient and wild-type mice was cut into 2-mm-thick tissue blocks, decontaminated in concentrated formic acid for 1 h, postfixed in 4% phosphate-buffered formalin by the method of Brown et al. (8), and embedded in paraffin. Brain sections (2 μm thick) were deparaffinized, rehydrated using xylene and a graded ethanol series, and first stained with hematoxylin and eosin.

For immunohistochemistry, antigen activity was enhanced by microwave treatment of sections for three 5-min intervals in 2 mM hydrochloric acid. Nonspecific binding was blocked with I-Block (Tropix; Applied Biosystems). The sections were then incubated for 90 min with the primary polyclonal antibody against the 14-3-3γ isoform (14-3-3-γ1005; dilution, 1:1,000) at room temperature, followed by a corresponding secondary alkaline phosphatase-conjugated antibody (goat anti-rabbit antibody [Dako]; dilution, 1:50) for 45 min. After neurofuchsin staining, the slides were counterstained with Haemalaun solution (Merck).

2D-DIGE. First-dimension isoelectric focusing was performed with immobilized pH 3 to 10 nonlinear gradient gels (24-cm Immobiline dry strips pH 3–10 NL; Amersham Biosciences). IPG strips were rehydrated for 24 h in 7 M urea–2 M thiourea–4% CHAPS–1% dithiothreitol (DTT)–0.4% IPG buffer pH 3–10 NL–0.002% bromophenol blue. Whole brain samples were dissolved in 3 volumes of ice-cold acetone and precipitated overnight at −20°C. Proteins were pelleted, air dried for 1 h, and lysed in 7 M urea–2 M thiourea–4% CHAPS–30 mM Tris-HCl (pH 8.1) for subsequent labeling. Insoluble material was removed by centrifugation. The proteins were labeled, as specified by the manufacturer, with fluorescent dyes specifically developed for the two-dimensional 2D difference gel electrophoresis system (2D-DIGE) (CyDyes Cy2, Cy3, and Cy5 [Amersham Biosciences]). Labeled samples were cup-loaded near the anodic end, and isoelectric focusing was carried out for a total of 56,000 Vh. After focusing, the strips were equilibrated for two 25-min intervals in 6 M urea–125 mM Tris-HCl (pH 7.85)–3% SDS–20 (vol/vol) glycerol; 1% DTT was added for the first equilibrium step, and 4.2% iodoacetamide (IAA) was added for the second equilibrium step. SDS-PAGE was performed with homogeneous 11% polyacrylamide gels (254 by 200 mm) by the method of Tastet et al. (37) at 20 W/gel. All gels were run in triplicate and analyzed with DeCyder differential analysis software (Amersham Biosciences). For subsequent mass spectrometry (MS), the proteins were stained with colloidal Coomassie blue by the method of Neuhoff et al. (28) and spots were excised manually.

Protein identification. Excised spots were subjected to manual or automatic in-gel digestion without prior alkylation, as specified in the protocols supplied with the ProTeam Digest system (Tecan). MS grade trypsin was purchased from Promega. For the acquisition of peptide mass fingerprints (PMF) by matrix-associated laser desorption-ionization–time-of-flight (MALDI-TOF) MS, the peptides extracted from the gel plugs were applied to a prestructured sample support (AnchorChip target; Bruker) coated with a thin layer of α-cyano-4-hydroxy-cinnamic acid (16). The target was inserted into a Bruker Ultraflex TOF/TOF instrument (35) and subjected to an automated analysis loop using external calibration. Database searches in the NCBInr protein sequence database restricted to the taxonomy *Mus musculus* were performed using the Mascot Software 2.0 from Matrix Science (30) with carboxamidomethylation of cysteines and oxidation of methionines as variable modifications. The monoisotopic mass tolerance was set to 100 ppm, and one missed cleavage was allowed. Samples not unambiguously identified by PMF were analyzed manually by MS/MS using the LIFT technology of the Ultraflex TOF/TOF instrument (35) to obtain sequence information for selected peptides (peptide fragment fingerprint). Database searches using combined PMF and MS/MS data sets were performed as described above, with the fragment mass tolerance set to 0.7 Da.

Inoculations. Mice were inoculated intraperitoneally (i.p.) with brain homogenate containing 3 or 6 log 50% lethal dose (LD_{50}) infectious units or intracerebrally (i.c.) with brain homogenate containing 3 × 5 or 3 × 2 log LD_{50} infectious units of RML (passage 5) scrapie prions prepared as described previously (9). The mice were monitored every second day, and scrapie was diagnosed on the basis of standard clinical criteria. The mice were killed on the day of onset of terminal clinical signs of scrapie. Numbers of infected control animals were 1 +/+ and 1 +/− at 3 × 5 log LD_{50} i.c., 4 +/+ and 1 +/− at 3 × 2 log LD_{50} i.c., 3 +/+ and 2 +/− at 6 log LD_{50} i.p., and 2 +/+ at 3 log LD_{50} i.p. Numbers of infected 14-3-3γ-deficient mice were 6 at 3 × 5 log LD_{50} i.c., 4 at 3 × 2 log LD_{50} i.c., 2 at 6 log LD_{50} i.p., and 5 at 3 log LD_{50} i.p.

RESULTS

Targeting of the murine 14-3-3γ gene. A 14-3-3γ-deficient mutant mouse line was generated by a classical knockout strategy. The replacement of a SpeI-SmaI genomic DNA fragment representing bp 5849078 to 5853467 (GeneID 22682) by the neomycin resistance cassette resulted in deletion of 14-3-3γ exon 2 (bp 5849248 to 5849901) (Fig. 1), which codes for bp 198 to 852 of the 14-3-3γ mRNA (NM_018871). This represents more than 88% of the 14-3-3γ coding sequence. Southern blot and/or PCR genotyping of offspring resulting from interbreeding of mice heterozygous for the 14-3-3γ deletion (Fig. 2A and B) showed that the respective genotypes (wild type +/+; heterozygous KO +/−; homozygous KO −/−) were present at the expected 1:2:1 Mendelian frequency.

Expression of 14-3-3 isoforms. The deletion of 14-3-3γ protein in the knockout mice was confirmed by Western blot analysis of brain homogenates from +/+, +/−, and −/− mice (Fig. 2C). By using a specific anti-14-3-3γ antiserum, no band was detected in the homozygous knockout animals. In heterozygous animals, 14-3-3γ levels were reduced to 78% of wild-type values. We also tested the expression levels of the β, ζ, ε, and η 14-3-3 isoforms in whole-brain homogenates but found no significant changes (Fig. 2C).

Immunohistochemical analyses failed to detect 14-3-3γ labelling in brains of the 14-3-3γ-deficient mice (Fig. 3B). The immunolabelling of wild-type mouse brains showed predominantly a neuronal cytoplasmatic staining. This can be seen, for example, in the pyramidal cell bodies in the CA1 region of the hippocampus (Fig. 3A).

Anatomy and cage behavior. Neither heterozygous animals of the F_1 generation nor homozygous knockout mice of the F_2 generation showed obvious phenotypic alterations. Examination of knockout animals revealed no differences in the morphology and histological characteristics of the cortex, cerebellum, heart, lungs, digestive organs, liver, kidneys, muscles, salivary glands, testis, skin, or lymphatic system. Cage behavior and life span were normal compared to those of control animals (data not shown).

Inoculation with pathological prion protein. To examine if there is a pathophysiological role of 14-3-3γ in prion disease, we infected mice with pathological prion protein. After i.c. or i.p. inoculation of knockout and heterozygous or wild-type control mice with 3 or 6 log LD_{50} (i.p.) or with 3 × 2 or 3 × 5 log LD_{50} (i.c.) of RML-infected brain homogenate, no significant trend for prolonged survival of 14-3-3γ-deficient mice was observed (Fig. 4). Histological examination of brain sections of terminally ill knockout and control mice revealed no differences in the lesion pattern (Fig. 5). As in uninfected knockout and wild-type mice, no differences in the expression

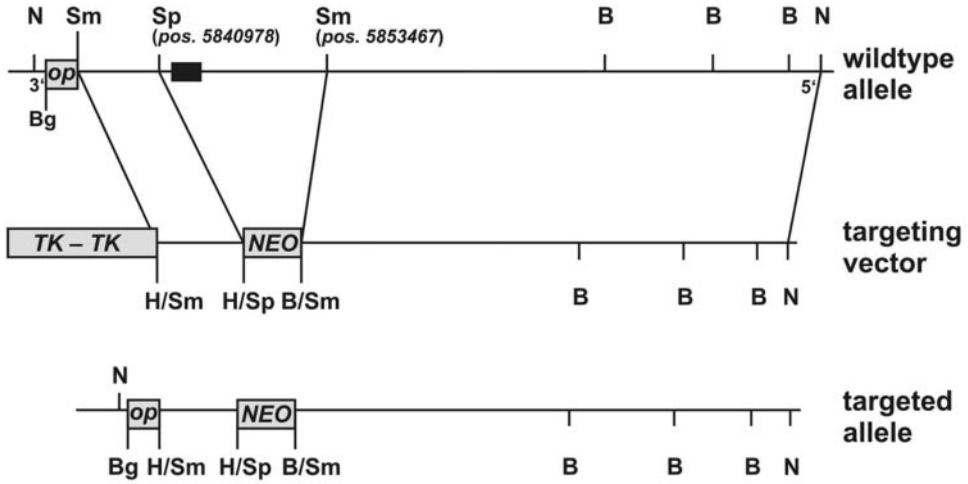

FIG. 1. Scheme of the 14-3-3γ knockout strategy. N, NotI; B, BamHI; Sm, SmaI; Sp, SpeI; Bg, BgIII; *op*, outside probe; *NEO*, neomycin resistance gene; *TK*, thymidine kinase gene. By sequencing of restriction fragments from the mouse genomic lambda insert (14-3-3γ; GeneID, 22628), more than 88% of the 14-3-3γ coding sequence was found to be located in the SpeI-SmaI fragment (bp 5849248 to 5849901). This 14-3-3γ exon 2 (bp 5849248 to 5849901) (indicated by a black box), including flanking regions between the SpeI and SmaI sites, was replaced by a neomycin resistance cassette in the targeting vector.

levels of the β, ζ, ε, and η 14-3-3 isoforms were detected by Western blot analysis (data not shown).

Candidate proteins. Since 14-3-3γ knockout mice display no obvious alterated phenotype, we characterized these mice in more detail. To analyze the levels of proteins that are reported to be binding partners of 14-3-3 proteins or to participate in the same signaling pathways, Western blot analyses were performed. We observed no significant up- or downregulation of BAD, Bcl2, phosphorylated Akt (pAkt), or total Akt, proteins involved in an apoptosis pathway. CDK5 and p35, proteins important in neuronal migration, were expressed at the same level as in the control brain homogenate. Several proteins involved in vesicle trafficking were quantified because 14-3-3γ was reported to bind phospholipids (29) and because 14-3-3 proteins are thought to be localized to synaptic vesicles, where they may promote Ca^{2+}-dependent exocytosis (18). In particular, SNAREs (SNAP-25, syntaxin, and synaptobrevin), SNARE-associated and regulatory proteins (complexin, synaptophysin, synaptotagmin, synaptojanin, synaptogyrin, Rab 3a, Rab-GDI, synapsin, *N*-ethylmaleimide-sensitive factor [NSF], and α-dynamin), and α-synuclein were examined. None of

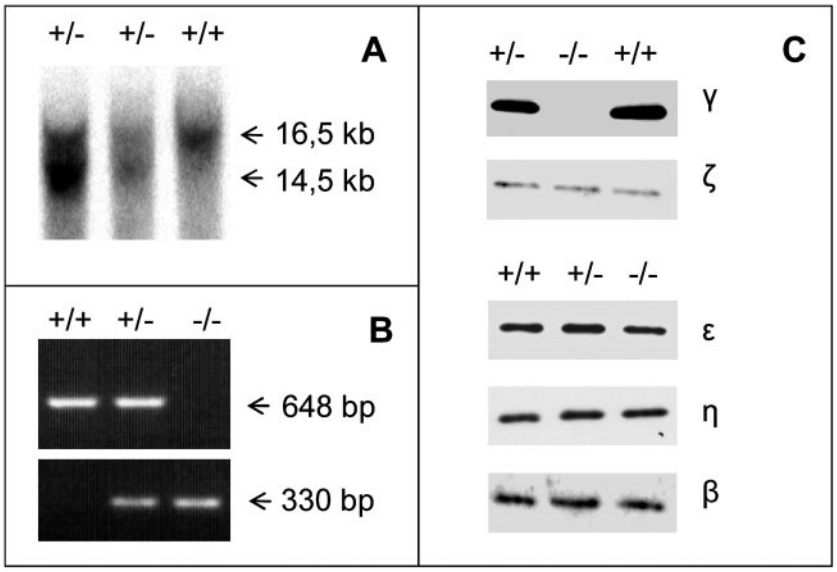

FIG. 2. (A) Southern blot of brain heart infusion-digested mouse genomic DNA, applying a 0.68-kb outside probe. Replacement of the genomic 4-kb SpeI-SmaI fragment results in a reduction of about 2 kb. (B) Genotyping by PCR. The 330-bp band is amplified by using two primers that bind in the neomycin resistance cassette. By applying two primers binding to the 14-3-3γ coding sequence, a PCR product of 648 bp is amplified. (C) Western blots of mouse brain homogenates, using specific antisera against the 14-3-3 isoforms γ, ε, β, ζ, and η.

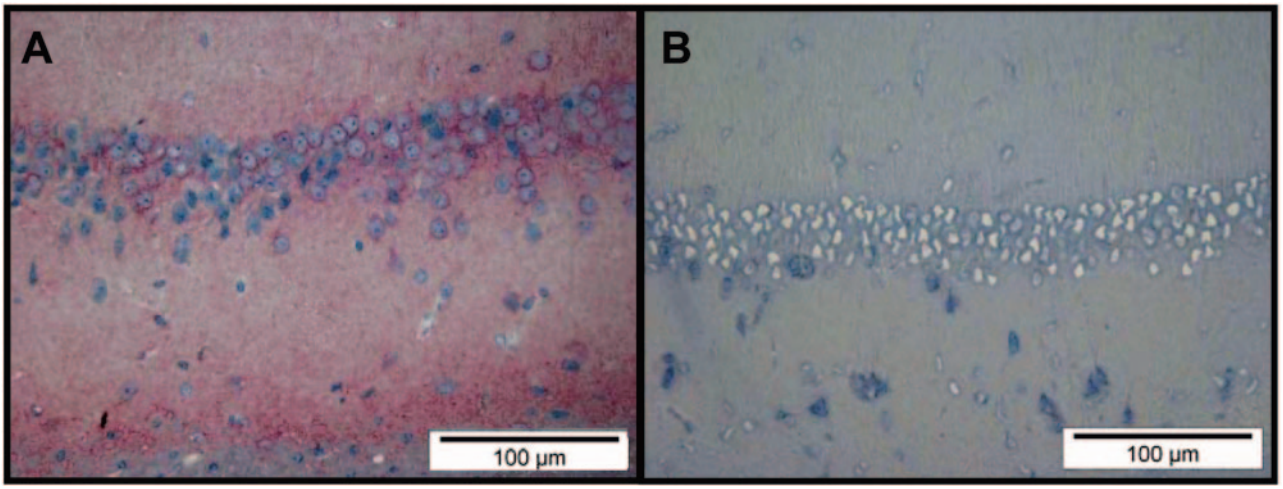

FIG. 3. 14-3-3γ labeling of the cell bodies in CA1 hippocampus in a normal murine brain (A) and a 14-3-3γ-deficient murine brain (B).

these proteins showed altered expression levels in 14-3-3γ-deficient mice (data not shown).

Proteomic analysis. Since our candidate protein approach did not reveal altered expression of the tested proteins, we next applied a more systematic proteomic approach. Using 2D-DIGE we investigated mixtures of total-brain homogenates from seven 12-week-old female 14-3-3γ knockout and wild-type control animals. Proteins showing different expression levels in the brain pool gels (Fig. 6A) were confirmed by 2D PAGE analysis of brains from individual mice, excised manually, and identified by MS. The proteins we found to be differentially expressed in the brains of 14-3-3γ knockout mice are listed in Table 1, and the corresponding spots are shown in Fig. 6B.

As demonstrated by the Western blots, 2D gels, and subsequent MS, our data verify the complete deletion of the 14-3-3γ isoform in mutant mice (Fig. 6B, panel III). Additionally, we were able to identify six proteins whose expression levels are differentially regulated in mutant mice (Fig. 6B; Table 1): growth hormone, the antioxidant protein 1-Cys peroxiredoxin, the zeta subunit (CCT-zeta-1) of T-complex protein 1 (a chaperone mediating protein folding), glucose-6-phosphate isomerase (a glycolytic enzyme that exhibits extracellular cytokine activity as an autocrine motility factor), the 170-kDa glucose-regulated protein GRP170 precursor (a molecular chaperone located in the endoplasmic reticulum that is induced mainly by glucose starvation and oxygen deprivation), and α-SNAP (a SNARE-associated cytosolic protein).

Discussion

In this paper we report on the generation and characterization of a 14-3-3γ-deficient mutant mouse line. The 14-3-3 protein family is characterized by widespread expression and high homology between isoforms and species. Seven mammalian isoforms with different subcellular localisation and function are known (2). 14-3-3 isoforms form homo- and heterodimers, bind to phosphorylated and nonphosphorylated motifs of a wide variety of target proteins, and are involved in diverse functions such as cell cycle control, apoptosis, and signal transduction (reviewed in references 2, 4, and 14). Recent reports emphasize that 14-3-3 proteins play a major role in protein-folding diseases (10, 46).

Our main reason for the generation of 14-3-3γ-deficient mutant mice was to test the hypothesis that 14-3-3 proteins play a pathophysiological role in prion diseases since the ap-

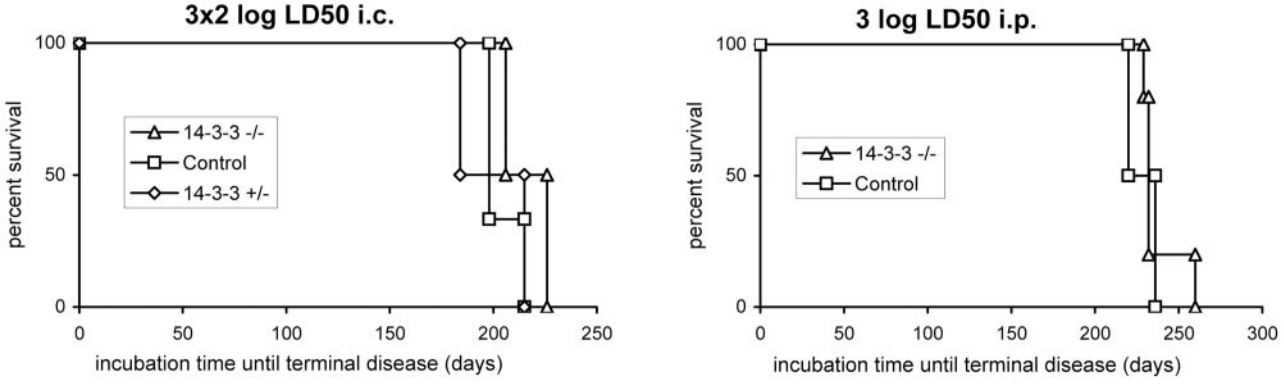

FIG. 4. Kaplan-Meier survival curves of mice inoculated either i.c. or i.p. with RML strain at 3 × 2 or 3 log LD_{50}, respectively.

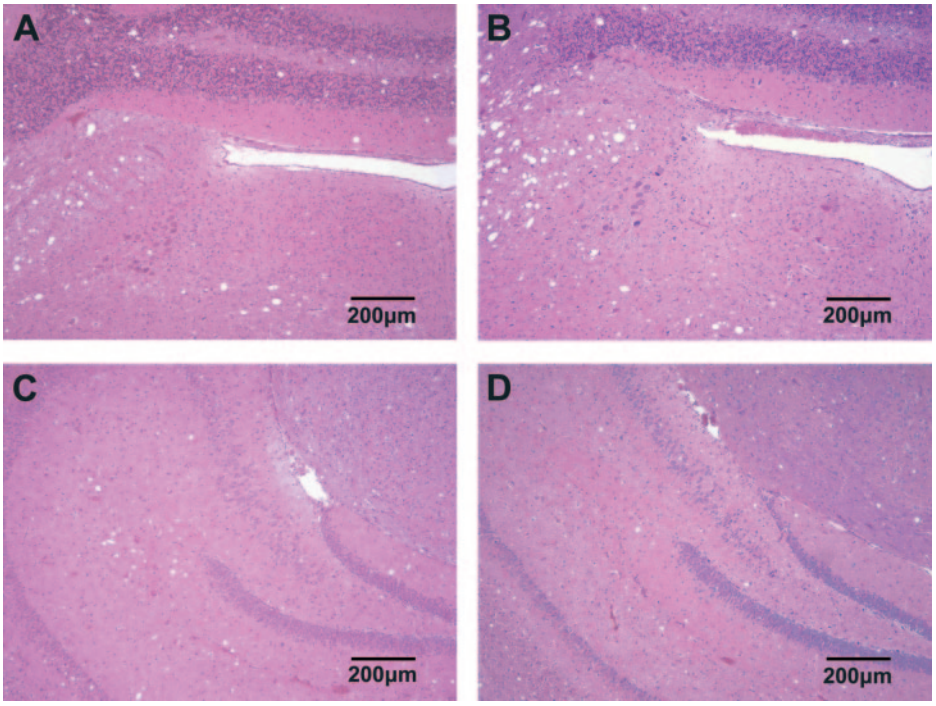

FIG. 5. Hematoxylin-eosin staining of brain samples from terminally ill 14-3-3γ knockout mice (A and C) and wild-type control mice (B and D) after inoculation with pathological prion protein (3 log LD_{50} of RML). (C and D) CA4, CA3, and parts of CA1 region of the hippocampus and the dentate gyrus; (A and B) brain stem at the level of the locus coeruleus with the fourth ventricle and cerebellar vermis.

pearance of 14-3-3 protein in cerebrospinal fluid supports the clinical diagnosis of CJD. By using isoform specific antisera, it was demonstrated that one 14-3-3 isoform (η) also appears in cerebrospinal fluid in other neurodegenerative diseases and dementias. Quantification of the γ, β, ε, and η isoforms can therefore be used to differentiate these diseases (45).

In the context of a possible role of 14-3-3γ in CJD, there were no differences in the survival times between 14-3-3γ mutant mice and control mice after i.c. or i.p. inoculation of strain RML. Since there was no significant increase in the expression levels of 14-3-3 isoform ε, β, ζ, or η in noninoculated and inoculated 14-3-3γ-deficient mice, a compensatory upregulation of other 14-3-3 isoforms is unlikely. However, it is possible that the endogenous levels of other 14-3-3 isoforms suffice to compensate for 14-3-3γ loss or that the changes in subcellular localization account for compensation. In any case, our results do not support the view of a direct involvement of 14-3-3γ in the pathogenesis of prion diseases. Rather, the 14-3-3 isoforms found in cerebrospinal fluid of CJD patients and animals with transmissible spongiform encephalopathies are more general markers of neurodestruction. The question why the spectrum of 14-3-3 isoforms in the brain differs from that observed in cerebrospinal fluid remains open. The most abundant 14-3-3 isoform, 14-3-3ζ, and its phosphorylated form (previously called δ [38]) appear to be absent from the cerebrospinal fluid of patients with CJD (45), but 14-3-3 ζ has been identified in amyloid plaques from patients with CJD (32). A possible role of 14-3-3 proteins has also been suggested in other neurodegenerative diseases. In Alzheimer's disease, 14-3-3 proteins were found in the neurofibrillary tangles (24), where they modulate the phosphorylation of tau protein (17). In Parkinson's disease and Lewy body disease, 14-3-3 ε, γ, and τ isoforms were found to bind to α-synuclein (4, 20, 42). A possible pathophysiological role of 14-3-3 proteins has also been discussed for Parkinson's disease, where, due to the increased expression of α-synuclein and the concomitant binding of 14-3-3 proteins, a reduction in the amount of free cytosolic antiapoptotic 14-3-3 protein appears to occur (46). In the polyglutamine disease spinocerebellar ataxia 1, 14-3-3 isoforms colocalize in ubiquitin-positive nuclear inclusions with ataxin-1. Recently, it was demonstrated that 14-3-3 isoforms ε and ζ bind and stabilize ataxin-1 and modulate its neurotoxicity, depending on the Akt-mediated phosphorylation status of ataxin-1 (10). For spinocerebellar ataxia 1, a chaperone suppression of ataxin-1 aggregation by HDJ/2HSDJ was shown (12), which represents the first example of chaperone involvement in polyglutamine disease. In Huntington's disease, perinuclear inclusions contain proteasomal proteins, α-synuclein, and 14-3-3 proteins in addition to Huntingtin protein (43). In amyotrophic lateral sclerosis, 14-3-3 was not only localized in neuronal aggregates but also found in glial cytoplasmic inclusions (15, 19).

These data indicate that 14-3-3 proteins might act as cochaperones or adapter proteins and be involved in the generation or stabilization of protein aggregates in a more general manner. While our present data show that this putative role of 14-3-3γ is not relevant in transmissible spongiform encephalopathies, it may well be important in one or more of the other neurodegenerative diseases for which a link to 14-3-3 proteins has been established. The mouse line described here is ideally suited for use in experiments to examine this possibility in corresponding mouse models of other neurodegenerative diseases—at least as far as the 14-3-3γ isoform is concerned.

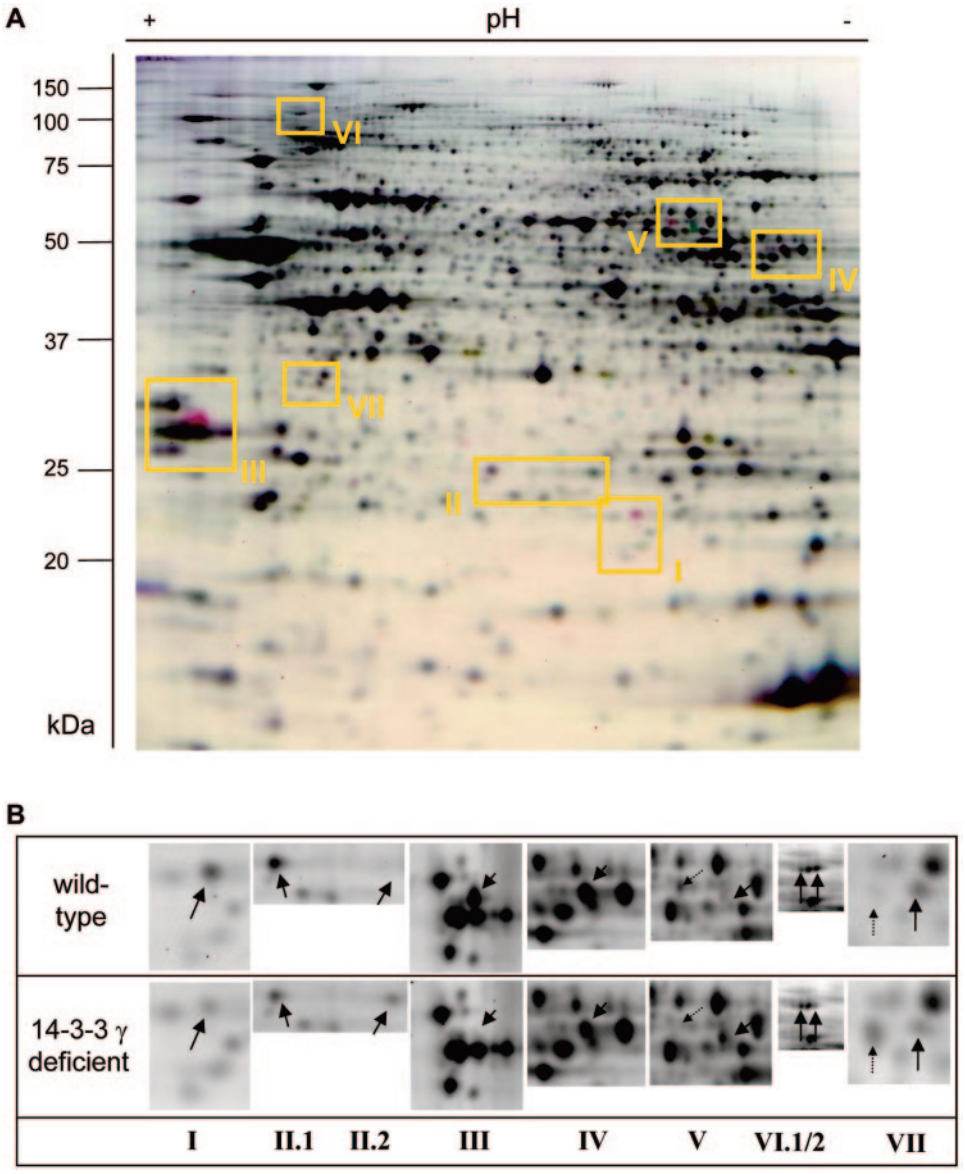

FIG. 6. (A) 2D PAGE of CyDye-labeled whole-brain proteins of pooled brains from seven 12-week-old female wild-type mice (red) and seven 14-3-3γ knockout mice (green). (B) Boxes I to VII show areas with differentially expressed proteins that were picked and identified by MS. Arrows indicate identified proteins (see Table 1). In boxes V and VII, arrows with dotted lines indicate differentially expressed proteins that are not yet identified.

The fact that 14-3-3γ knockout mice do not show any obvious phenotypic changes leads to the assumption that other proteins have taken over the role of 14-3-3γ. To examine this in more detail, we extended the characterization of 14-3-3γ knockout mice by using a hypothesis driven and a proteomic approach.

For a 14-3-3ε deletion mutant mouse, hippocampal defects and thinning of the cortex were reported (39). Neuronal migration in these mice is defective. In addition, 14-3-3ε binds to CDK5/p35 phosphorylated NUDEL, prevents its dephosphorylation, and thus influences its subcellular localization (39). 14-3-3γ was also found to bind NUDEL in yeast-two-hybrid assays (39). If there is a real functional involvement of 14-3-3γ in this process of neuronal migration, it could not be proven by using our mutant mouse. It is possible that 14-3-3ε can replace 14-3-3γ in this process. However this isoform was not upregulated in our mutant mouse.

Since 14-3-3γ is known to bind phospholipids (33) and 14-3-3 proteins were implicated in exocytosis (7, 27), we analysed key proteins involved in vesicle trafficking and fusion. We observed no differences between 14-3-3γ-deficient and control mice. We also examined proteins involved in apoptosis regulation, including BAD, which is a binding partner of 14-3-3 (47). Again, no differences in protein expression levels were observed.

Further information was obtained by a proteomic approach. 2D-DIGE analyses revealed several differentially expressed proteins. Six of these proteins have now been identified by MS.

TABLE 1. List of identified proteins that are differentially expressed in wild-type and 14-3-3γ knockout mice

Protein	Name	Accession no.	Theoretical mol wt	No. of peptides matched	Sequence coverage (%)	Mowse score[a]
I	Growth hormone	gi|38173967	24,700	5	23	116*
II.1	1-Cys peroxiredoxin protein	gi|4139186	24,825	7	40	73
II.2	1-Cys peroxiredoxin protein	gi|4139186	24,825	8	47	116
III	14-3-3 protein gamma	gi|3065929	28,344	10	42	93
IV	T-complex protein 1, zeta subunit (CCT-zeta-1)	gi|549061	57,967	8	19	137*
V	Glucose-6-phosphate isomerase (GPI)	gi|120741	62,728	17	27	121
VI.1	170-kDa glucose-regulated protein GRP170 precursor	gi|7643979	111,112	19	24	156
VI.2	170-kDa glucose-regulated protein GRP170 precursor	gi|7643979	111,112	17	20	149
VII	*N*-Ethylmaleimide-sensitive fusion protein attachment protein alpha	gi|13385392	33,168	8	36	107*

[a] Mowse scores were obtained by peptide mass fingerprinting or (marked by asterisks) additional peptide fragment fingerprinting.

Further detailed analyses of these proteins and the pathways in which they are involved will have to be carried out to elucidate why these proteins are differentially expressed in 14-3-3γ deletion mutant mice.

However, for some of these differentially regulated proteins, a functional link to 14-3-3γ may exist. α-SNAP, for example, is required for intracellular membrane trafficking. It binds to syntaxin and recruits NSF to SNARE complexes. Another presynaptic protein which was reported to bind 14-3-3 is Rim1, a brain-specific rab3a binding protein and modulator of SNARE function and exocytosis (36). In *Caenorhabditis elegans*, Rim1/UNC-10 probably acts to regulate the priming step of presynaptic vesicle fusion by promoting conformational changes in syntaxin (21). Also CCT zeta, another differentially expressed protein, which is part of a molecular chaperone TCP1 complex, has been reported to be involved in vesicular trafficking (11).

GRP170 precursor protein is located at the endoplasmic reticulum (ER) and is induced by ER stresses that are caused by the accumulation of unfolded or immature proteins in the ER and the decelerated protein trafficking via the ER (34). The γ isoform of 14-3-3 proteins is the major isoform in the Golgi complex and is implicated in secretion and protein trafficking (reviewed in reference 2). 1-Cys peroxiredoxin, an antioxidant protein, was also shown to be differentially regulated. In 14-3-3γ knockout mice, this peroxidase is shifted to a more acidic pI that corresponds to overoxidation of the active-site cysteine into cysteine sulfinic acid (44). The same was found in heart cells of PKC-δ knockout mice (26). Interestingly, CCT zeta was also differentially expressed in the hearts of these mice (26).

Taken together, further characterization of 14-3-3γ deletion mutant mice under different experimental settings should lead to a greater understanding of the cellular function of the 14-3-3 isoform and, as discussed above, a possible role in other — nontransmissible pongiform encephalopathy—protein-folding diseases.

ACKNOWLEDGMENTS

This study was supported by grants from the European Union (CT98-6016), the German Ministry of Health and Social Security (BMGS), and the Center for Molecular Physiology of the Brain (CMPB-DFG Research Center).

REFERENCES

1. **Aitken, A.** 2002. Functional specificity in 14-3-3 isoform interactions through dimer formation and phosphorylation. Chromosome location of mammalian isoforms and variants. Plant Mol. Biol. **50:**993–1010.
2. **Aitken, A., H. Baxter, T. Dubois, S. Clokie, S. Mackie, K. Mitchell, A. Peden, and E. Zemlickova.** 2002. Specificity of 14-3-3 isoform dimer interactions and phosphorylation. Biochem. Soc. Trans. **30:**351–360.
3. **Baxter, H. C., J. R. Fraser, W. G. Liu, J. L. Forster, S. Clokie, P. Steinacker, M. Otto, E. Bahn, J. Wiltfang, and A. Aitken.** 2002. Specific 14-3-3 isoform detection and immunolocalization in prion diseases. Biochem. Soc. Trans. **30:**387–391.
4. **Berg, D., C. Holzmann, and O. Riess.** 2003. 14-3-3 proteins in the nervous system. Nat. Rev. Neurosci. **4:**752–762.
5. **Berg, D., O. Riess, and A. Bornemann.** 2003. Specification of 14-3-3 proteins in Lewy bodies. Ann. Neurol. **54:**135.
6. **Boston, A., P. Jackson, and R. J. Thompson.** 1982. Human 14-3-3 protein: radioimmunoassay, tissue distribution, and cerebrospinal fluid levels in patients with neurological disorders. J. Neurochem. **38:**1475–1482.
7. **Broadie, K., E. Rushton, E. M. Skoulakis, and R. L. Davis.** 1997. Leonardo, a *Drosophila* 14-3-3 protein involved in learning, regulates presynaptic function. Neuron **19:**391–402.
8. **Brown, P., A. Wolff, and D. C. Gajdusek.** 1990. A simple and effective method for inactivating virus infectivity in formalin-fixed tissue samples from patients with Creutzfeldt-Jakob disease. Neurology **40:**887–890.
9. **Büeler, H. R., A. Aguzzi, A. Sailer, R. A. Greiner, P. Autenried, M. Aguet, and C. Weissmann.** 1993. Mice devoid of PrP are resistant to scrapie. Cell **73:**1339–1347.
10. **Chen, H. K., P. Fernandez-Funez, S. F. Acevedo, Y. C. Lam, M. D. Kaytor, M. H. Fernandez, A. Aitken, E. M. Skoulakis, H. T. Orr, J. Botas, and H. Y. Zoghbi.** 2003. Interaction of Akt-phosphorylated ataxin-1 with 14-3-3 mediates neurodegeneration in spinocerebellar ataxia type 1. Cell **113:**457–468.
11. **Creutz, C. E., A. Liou, S. L. Snyder, A. Brownawell, and K. Willison.** 1994. Identification of the major chromaffin granule-binding protein, chromobindin A, as the cytosolic chaperonin CCT (chaperonin containing TCP-1). J. Biol. Chem. **269:**32035–32038.
12. **Cummings, C. J., M. A. Mancini, B. Antalffy, D. B. DeFranco, H. T. Orr, and H. Y. Zoghbi.** 1998. Chaperone suppression of aggregation and altered subcellular proteasome localization imply protein misfolding in SCA1. Nat. Genet. **19:**148–154.
13. **Fountoulakis, M., N. Cairns, and G. Lubec.** 1999. Increased levels of 14-3-3 gamma and epsilon proteins in brain of patients with Alzheimer's disease and Down syndrome. J. Neural Transm. Suppl. **57:**323–335.
14. **Fu, H., R. R. Subramanian, and S. C. Masters.** 2000. 14-3-3 proteins: structure, function, and regulation. Annu. Rev. Pharmacol. Toxicol. **40:**617–647.
15. **Giasson, B. I., M. E. Mabon, J. E. Duda, T. J. Montine, D. Robertson, H. I. Hurtig, V. M. Lee, and J. Q. Trojanowski.** 2003. Tau and 14-3-3 in glial cytoplasmic inclusions of multiple system atrophy. Acta Neuropathol. **106:** 243–250.
16. **Gobom, J., M. Schuerenberg, M. Mueller, D. Theiss, H. Lehrach, and E. Nordhoff.** 2001. Alpha-cyano-4-hydroxycinnamic acid affinity sample preparation. A protocol for MALDI-MS peptide analysis in proteomics. Anal. Chem. **73:**434–438.

17. **Hashiguchi, M., K. Sobue, and H. K. Paudel.** 2000. 14-3-3zeta is an effector of tau protein phosphorylation. J. Biol. Chem. **275:**25247–25254.
18. **Jones, D. H., H. Martin, J. Madrazo, K. A. Robinson, P. Nielsen, P. H. Roseboom, Y. Patel, S. A. Howell, and A. Aitken.** 1995. Expression and structural analysis of 14-3-3 proteins. J. Mol. Biol. **245:**375–384.
19. **Kawamoto, Y., I. Akiguchi, S. Nakamura, and H. Budka.** 2002. Accumulation of 14-3-3 proteins in glial cytoplasmic inclusions in multiple system atrophy. Ann. Neurol. **52:**722–731.
20. **Kawamoto, Y., I. Akiguchi, S. Nakamura, Y. Honjyo, H. Shibasaki, and H. Budka.** 2002. 14-3-3 proteins in Lewy bodies in Parkinson disease and diffuse Lewy body disease brains. J. Neuropathol. Exp. Neurol. **61:**245–253.
21. **Koushika, S. P., J. E. Richmond, G. Hadwiger, R. M. Weimer, E. M. Jorgensen, and M. L. Nonet.** 2001. A post-docking role for active zone protein Rim. Nat. Neurosci. **4:**997–1005.
22. **Kretzschmar, H. A., J. W. Ironside, S. J. DeArmond, and J. Tateishi.** 1996. Diagnostic criteria for sporadic Creutzfeldt-Jakob disease. Arch. Neurol. **53:**913–920.
23. **Laemmli, U. K.** 1970. Cleavage of structural proteins during the assembly of the head of bacteriophage T4. Nature **227:**680–685.
24. **Layfield, R., J. Fergusson, A. Aitken, J. Lowe, M. Landon, and R. J. Mayer.** 1996. Neurofibrillary tangles of Alzheimer's disease brains contain 14-3-3 proteins. Neurosci. Lett. **209:**57–60.
25. **Malaspina, A., N. Kaushik, and J. de Belleroche.** 2000. 14-3-3 mRNA is up-regulated in amyotrophic lateral sclerosis spinal cord. J. Neurochem. **75:**2511–2520.
26. **Mayr, M., Y. L. Chung, U. Mayr, E. McGregor, H. Troy, G. Baier, M. Leitges, M. J. Dunn, J. R. Griffiths, and Q. Xu.** 2004. Loss of PKC-delta alters cardiac metabolism. Am. J. Physiol. Ser. H. **287:**H937–H945.
27. **Morgan, A., and R. D. Burgoyne.** 1992. Exo1 and Exo2 proteins stimulate calcium-dependent exocytosis in permeabilized adrenal chromaffin cells. Nature **355:**833–836.
28. **Neuhoff, V., N. Arold, D. Taube, and W. Ehrhardt.** 1988. Improved staining of proteins in polyacrylamide gels including isoelectric focusing gels with clear background at nanogram sensitivity using Coomassie Brilliant Blue G-250 and R-250. Electrophoresis **9:**255–262.
29. **Patel, Y., H. Martin, S. Howell, D. Jones, K. Robinson, and A. Aitken.** 1994. Purification of 14-3-3 protein and analysis of isoforms in chicken brain. Biochim. Biophys. Acta **1222:**405–409.
30. **Perkins, D. N., D. J. Pappin, D. M. Creasy, and J. S. Cottrell.** 1999. Probability-based protein identification by searching sequence databases using mass spectrometry data. Electrophoresis **20:**3551–3567.
31. **Peyril, A., R. Weitzdoerfer, T. Gulesserian, M. Fountoulakis, and G. Lubec.** 2002. Aberrant expression of signaling-related proteins 14-3-3 gamma and RACK1 in fetal Down syndrome brain (trisomy 21). Electrophoresis **23:**152–157.
32. **Richard, M., A. G. Biacabe, N. Streichenberger, J. W. Ironside, M. Mohr, N. Kopp, and A. Perret-Liaudet.** 2003. Immunohistochemical localization of 14.3.3 zeta protein in amyloid plaques in human spongiform encephalopathies. Acta Neuropathol. **105:**296–302.
33. **Roth, D., A. Morgan, H. Martin, D. Jones, G. J. Martens, A. Aitken, and R. D. Burgoyne.** 1994. Characterization of 14-3-3 proteins in adrenal chromaffin cells and demonstration of isoform-specific phospholipid binding. Biochem. J. **301:**305–310.
34. **Sidrauski, C., R. Chapman, and P. Walter.** 1998. The unfolded protein response: an intracellular signalling pathway with many surprising features. Trends Cell Biol. **8:**245–249.
35. **Suckau, D., A. Resemann, M. Schuerenberg, P. Hufnagel, J. Franzen, and A. Holle.** 2003. A novel MALDI LIFT-TOF/TOF mass spectrometer for proteomics. Anal. Bioanal. Chem. **376:**952–965.
36. **Sun, L., M. A. Bittner, and R. W. Holz.** 2003. Rim, a component of the presynaptic active zone and modulator of exocytosis, binds 14-3-3 through its N terminus. J. Biol. Chem. **278:**38301–38309.
37. **Tastet, C., P. Lescuyer, H. Diemer, A. van Dorsselaer, and T. Rabilloud.** 2003. A versatile electrophoresis system for the analysis of high- and low-molecular-weight proteins. Electrophoresis **24:**1787–1794.
38. **Toker, A., L. A. Sellers, B. Amess, Y. Patel, A. Harris, and Aitken, A.** 1992. Multiple isoforms of a protein kinase C inhibitor (KCIP-1/14-3-3) from sheep brain: amino acid sequence of phosphorylated forms. Eur. J. Biochem. **206:**453–461.
39. **Toyo-oka, K., A. Shionoya, M. J. Gambello, C. Cardoso, R. Leventer, H. L. Ward, R. Ayala, L. H. Tsai, W. Dobyns, D. Ledbetter, S. Hirotsune, and A. Wynshaw-Boris.** 2003. 14-3-3epsilon is important for neuronal migration by binding to NUDEL: a molecular explanation for Miller-Dieker syndrome. Nat. Genet. **34:**274–285.
40. **Tsutsumi, S., V. Hogan, I. R. Nabi, and A. Raz.** 2002. Overexpression of the autocrine motility factor/phosphoglucose isomerase induces transformation and survival of NIH-3T3 fibroblasts. Cancer Res. **63:**242–249.
41. **Tzivion, G., and J. Avruch.** 2002. 14-3-3 proteins: active cofactors in cellular regulation by serine/threonine phosphorylation. J. Biol. Chem. **277:**3061–3064.
42. **Ubl, A., D. Berg, C. Holzmann, R. Kruger, K. Berger, T. Arzberger, A. Bornemann, and O. Riess.** 2002. 14-3-3 protein is a component of Lewy bodies in Parkinson's disease-mutation analysis and association studies of 14-3-3 eta. Brain Res. Mol. Brain Res. **108:**33–39.
43. **Waelter, S., A. Boeddrich, R. Lurz, E. Scherzinger, G. Lueder, H. Lehrach, and E. E. Wanker.** 2001. Accumulation of mutant huntingtin fragments in aggresome-like inclusion bodies as a result of insufficient protein degradation. Mol. Biol. Cell **12:**1393–1407.
44. **Wagner, E., S. Luche, L. Penna, M. Chevallet, A. Van Dorsselaer, E. Leize-Wagner, and T. Rabilloud.** 2002. A method for detection of overoxidation of cysteines: peroxiredoxins are oxidized in vivo at the active-site cysteine during oxidative stress. Biochem. J. **366:**777–785.
45. **Wiltfang, J., M. Otto, H. C. Baxter, M. Bodemer, P. Steinacker, E. Bahn, I. Zerr, J. Kornhuber, H. A. Kretzschmar, S. Poser, E. Rüther, and A. Aitken.** 1999. Isoform pattern of 14-3-3 proteins in the cerebrospinal fluid of patients with Creutzfeldt-Jakob disease. J. Neurochem. **73:**2485–2490.
46. **Xu, J., S. Y. Kao, F. J. Lee, W. Song, L. W. Jin, and B. A. Yankner.** 2002. Dopamine-dependent neurotoxicity of alpha-synuclein: a mechanism for selective neurodegeneration in Parkinson disease. Nat. Med. **8:**600–606.
47. **Zha, J., H. Harada, E. Yang, J. Jockel, and S. J. Korsmeyer.** 1996. Serine phosphorylation of death agonist BAD in response to survival factor results in binding to 14-3-3 not BCL-X(L). Cell **87:**619–268.